Title
Coordinate control of air movement for optimal thermal comfort

Authors
Liu, Shuo
Yin, Le
Schiavon, Stefano
et al.

Publication Date
2018-04-02

DOI
10.1080/23744731.2018.1452508

Peer reviewed

Coordinate control of air movement for optimal thermal comfort

LIU Shuo [1,2], YIN Le [3*] , SCHIAVON Stefano [4], HO Weng Khuen [2], LING Keck Voon [3]

[1] *Berkeley Education Alliance for Research in Singapore, Singapore 138602*

[2] *Department of Electrical and Computer Engineering, National University of Singapore, Singapore 119077*

[3] *School of Electrical and Electronic Engineering, Nanyang Technological University, Singapore 639798*

[4] *Center for the Built Environment, University of California, Berkeley, CA 94720, USA*

*Corresponding author. *E-mail address*: yinl0002@e.ntu.edu.sg

Abstract

Personally controlled air movement can maintain or enhance thermal comfort in warm environments and reduce energy consumption. Unlike controlling a personal fan, using a system of fans for multiple occupants is difficult as it is hard to find an appropriate fan speed setting that maximizes occupants' satisfaction. Since limited work has been carried out on this issue, in this paper, a novel cooperative control approach for a system of fans is proposed to provide optimized air movement for multiple occupants. This is the first time that a system of fans is controlled cooperatively in the research of built environment. The proposed approach predicts airflow in a cost-effective manner by calibrating the fans in the real environment. The operation of the fans is optimized by minimizing the worst-case deviation between the actual air speed and the desired air speed, which can be determined based on either the PMV – SET model or the occupants' feedback. This minimax-error problem is formulated as an equivalent linear programming problem which can be solved using standard methods. The proposed approach was tested in two different indoor scenarios respectively by 1) measuring air speed directly in a business conference room and 2) involving human subject surveys in a university classroom. In the first experiment, the measured air speeds after optimization are closer to the target values at all tested temperature levels (26 °C, 27.5 °C and 29 °C) indicating improved thermal comfort. In the second experiment, only 62% of the occupants (totally 34) are satisfied with slightly increased room temperature (around 26.5 °C) before optimization, while this number increased to 94% after optimization.

1. Introduction

Nowadays, a large percentage of global energy consumption is attributed to buildings. Studies have found that the building sector accounts for about 37% of total energy consumption in the EU, about 39% in the UK (Pérez-Lombard et al. 2008), about 41% in the US (DOE 2011) and about 51% of total electricity usage in Singapore (EMA 2015). For end use, the heating, ventilation and air conditioning (HVAC) system has been found to contribute to the largest building energy consumption, namely, about 47% in the US (DOE 2011). In the tropics such as Singapore, 50% of building electricity usage is consumed by air conditioning (NEA 2010).

 https://doi:10.1080/23744731.2018.1452508
www.escholarship.org/uc/item/0m91d1t2

Increasing cooling setpoint of the air conditioning system in a building allows energy savings (Sekhar 1995, Schiavon & Melikov 2008, Hoyt et al. 2015, Rim et al. 2015, Duarte et al. 2016) but a balance is always necessarily required between energy efficiency and thermal comfort (Kolarik et al. 2011, Khalil & Abou Zeid 2016, Shahzad et al. 2017). Air movement at elevated air speed generated by electric fans can be used to compensate the impact brought by the increased temperature on thermal comfort. Many studies have shown that great demand for air movement is required indoors (Cândido et al. 2011, Huang et al. 2013, Yang & Olofsson 2017) and personally controlled air movement can maintain human thermal comfort in warm environments (Zhai et al. 2013, Yang et al. 2015, Schiavon et al. 2017). Thermal comfort standards such as ASHRAE 55 (ANSI/ASHRAE 2013) also support the use of increased air movement in the design of buildings. However, fans are still not commonly used in commercial buildings, even though the potential for thermal comfort improvement and energy conservation has been verified.

Our previous studies have found that joint utilization of electric fan and air conditioning system would significantly reduce building energy consumption because of increased cooling setpoints. A simulation study of a benchmark office building in Singapore (Duarte et al. 2016) shows that a 3 °C increase in zone temperatures from baseline 23 °C would correspond to about 17% savings in the air conditioning mechanical ventilation (ACMV) system. In the meanwhile, the overall energy consumption increases only 0.7% when fans are used for maintaining thermal comfort. In addition to focusing on the outright energy savings, we also demonstrate in (Xu et al. 2017) that coordinating air conditioning system and fans can enhance the demand response (DR) capability and thermal storage capacity in buildings.

The methods for controlling a personal fan to deliver thermal comfort have been developed in (Cheng 1993, Gluszek & Gluszek 1995, Liu et al. 2017). However, limited work has been carried out for the optimal operation of a plurality of fans. Unlike controlling a personal fan, using a system of fans for multiple occupants is difficult as it is usually hard to find an appropriate fan speed setting that maximizes users' satisfaction. There are several reasons for this. Firstly, fans commonly generate a strongly non-uniform air speed distribution. The assumption of a homogeneous air speed distribution generated by fans is incorrect. Secondly, thermal environment is spatially non-uniform and temporally unsteady. People sitting at different positions may be exposed to different environmental conditions. Thirdly, people have different thermal preferences. This individual difference among occupants should be considered in the operation of fans. Fourth, the configuration of the fans (e.g., number of fans and their placements) and their operation are not optimized. Occupants may experience too weak or too strong airflow. Fifth, occupancy distribution changes from time to time. If the fan speed setting is not updated according to occupancy changes, wasted energy and suboptimal thermal comfort may happen. As a consequence, there will always be different opinions among the users regarding the fan speed setting. When someone adjusts the fans to suit him/herself, it is highly possible that other people may feel uncomfortable. This problem can be solved if fans are cooperatively controlled by taking into account the preferences of the occupants and variation of environmental conditions.

In this paper, a cooperative control approach is proposed for a system of fans to provide optimized air movement for multiple occupants thereby improving thermal comfort and saving energy. To the best of authors' knowledge, this is the first time that a system of fans is controlled cooperatively to maximize users' satisfaction. Conventionally, airflow is usually predicted based

on the simulation results obtained from the Computational Fluid Dynamics (CFD) software. However, the proposed approach predicts airflow in a cost-effective manner by calibrating the fans in real environments to establish the relationship between air speed and fan speed setting. In addition, the operation of the fans is optimized to minimize the worst-case deviation between the actual air speed and the desired air speed by using linear programming algorithm.

Two methods to determine the desired air speed are employed. The first method is to measure environmental conditions and calculate the desired air speed based on the PMV – SET (Predicted Mean Vote – Standard Effective Temperature) model (Arens et al. 2009, Schiavon et al. 2014). Since the PMV human heat balance model underestimates the influence of air movement, Arens et al. (2009) merged the PMV model with the SET index, which is based on Gagge's (1971) two-node model of human temperature regulation, to set a comfort zone at elevated air speed. The PMV – SET model is based on the idea that equal heat balance and skin wettedness for different air speeds can be plotted in terms of SET contours. Each contour is a curve over a range of dry-bulb temperature, mean radiant temperature and air speed such that every point on this curve produces the same SET value (Arens et al. 2009). The model has been adopted by ASHRAE Standard 55-2013 (ANSI/ASHRAE 2013). This is a passive-design approach by measuring the environmental variable such as air temperature. Personalization and customization can be provided by setting different target PMV values for different persons upon their requirements. Alternatively, the desired value of air speed can also be determined according to the real-time feedback (e.g., short message service, smartphone app or network graphical user interface) from the occupants regarding their preferences of air movement

2. Methods

2.1 System overview

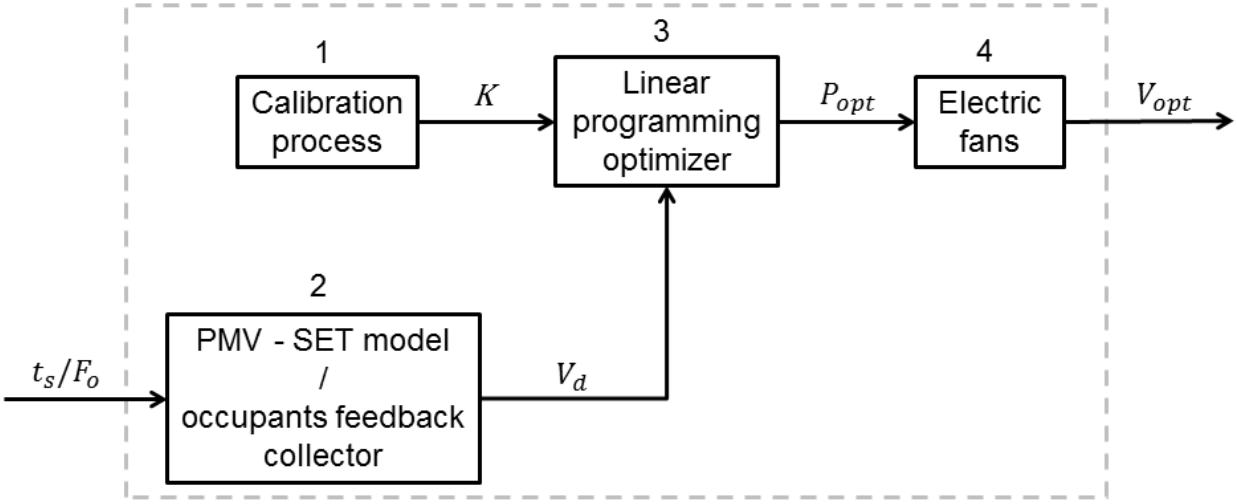

Figure 1: Steps to generate the optimized air speed.

The whole process of the proposed approach is shown in Figure 1. The input to the system can be either the sensed environmental parameters (e.g., dry-bulb air temperature, t_s) or the collected occupants feedback, F_o, depending on the chosen method of desired air speed determination. The output is the optimized air speeds, V_{opt}, generated by the electric fans to which the optimal fan speed setting, P_{opt}, are applied. The four steps in Figure 1 are explained as follows:

Step 1: Calibration. The calibration process is to determine the gain of the air speed to the fan speed setting, *K*, at target positions or zones. These positions or zones are located where the occupants are expected to be.

Step 2: Determination of desired air speed. The desired air speed, V_d, can be determined based on either the PMV – SET thermal comfort model by estimating the PMV input parameters or the real-time feedback from the occupants which indicates their preference of air movement.

Step 3: Optimization. The proposed approach considers the deviations of the actual air speed from the desired air speed for all the occupants, and then cooperatively controls the system of fans to obtain the optimized fan speed setting P_{opt} by minimizing the worst-case deviation through linear programming.

Step 4: Output. The optimized fan speed setting P_{opt} from Step 3 are then applied to the electric fans to provide optimized air speed V_{opt} at target positions or zones.

Experiments have been conducted to prove the concept and feasibility of the proposed approach. In the experiments, three-phase brushless direct current (DC) fans (Model FSAW98RI-A, Airmate, China) were employed. Each fan consumes only 3.8 W to 32.5 W depending on the fan speed setting applied (Table A.1 in Supplementary Information). The fan power was measured by a power meter (Energy monitoring socket, Efergy, UK) with an accuracy of ± 2% of readings. The air speed was measured by an air distribution measuring system (AirDistSys5000, Sensor Electronics, Poland) equipped with omnidirectional air speed sensors (SensoAnemo 5100SF, Sensor Electronics, Poland). Each sensor provides an accuracy of 0.02 m/s for the air speed in the range of 0.05 m/s to 5 m/s. Air temperature and relative humidity were recorded by HOBO data loggers (Model U12-013, Onset, USA) with ±0.35 °C uncertainty for air temperature and ±2.5% uncertainty for relative humidity.

2.2 Optimization of Fans Operation

2.2.1 Problem Formulation

In practice, personal control over the fans may not be available since the number of fans can be smaller than that of people. As a consequence, not everyone can have her/his desired airflow. Therefore, we need to select a fan speed setting that is optimal with respect to some criteria. As thermal dissatisfaction grows non-linearly when a deviation from the comfort condition increases (Fanger 1970), the minimax-error criterion that aims at limiting the maximum error within an acceptable range is employed. For example, if the initial deviations from the desired air speed for three occupants are 0.1 m/s, 0.2 m/s and 0.3 m/s, then the worst case is 0.3 m/s and the goal is to reduce the worst case as much as possible. The problem of optimizing fans operation is therefore formulated as to find the optimal fan speed setting P_{opt} that minimizes the maximum absolute error between the actual air speed *V(P)* and the desired air speed V_d, i.e.

$$\text{Minimize } ||V(P) - V_d||_\infty \tag{1}$$

where *P* is the speed setting applied to the fans and V_d can be obtained based on the PMV – SET model or the feedback from occupants. The relationship between *V(P)* and *P* is assumed to be linear or approximately linear. This assumption is verified experimentally for the selected DC fan and the results are given in Supplementary Information (Figure A.1 and Table A.2). For the nonlinear case, numerical optimization can be performed via linearization, which will be described in Section 2.2.3.

2.2.2 Minimax-error solution and linear programming

A. A simple example

Before discussing the general case, we first give the mathematics for a simple example of one fan with speed setting p and two occupants with desired air speeds v_{d1} and v_{d2}. Let the actual air speeds at the two positions due to the fan be given by

$$v_1 = k_1 p \tag{2}$$

$$v_2 = k_2 p \tag{3}$$

where k_1 and k_2 are gains of v_1 and v_2 with respect to p, respectively. Let the absolute errors between the actual air speed and the desired air speed be less than or equal to the maximum error, ε, which we want to minimize, the following inequalities can be obtained

$$|v_{d1} - v_1| \leq \varepsilon \tag{4}$$

$$|v_{d2} - v_2| \leq \varepsilon \tag{5}$$

Removing the modulus sign in inequalities (4) and (5) gives

$$v_1 - v_{d1} \leq \varepsilon \tag{6}$$

$$v_2 - v_{d2} \leq \varepsilon \tag{7}$$

$$v_{d1} - v_1 \leq \varepsilon \tag{8}$$

$$v_{d2} - v_2 \leq \varepsilon \tag{9}$$

Substituting Eqs.(2) and (3) into inequalities (6) to (9) and rearranging give

$$\begin{bmatrix} k_1 & -1 \\ k_2 & -1 \\ -k_1 & -1 \\ -k_2 & -1 \end{bmatrix} \begin{bmatrix} p \\ \varepsilon \end{bmatrix} \leq \begin{bmatrix} v_{d1} \\ v_{d2} \\ -v_{d1} \\ -v_{d2} \end{bmatrix} \tag{10}$$

The optimal speed setting p_{opt} that minimizes the maximum error ε can then be obtained by solving the following linear programming problem (Norman 1991):

$$\text{Minimize } [0 \quad 1] \begin{bmatrix} p \\ \varepsilon \end{bmatrix} \tag{11}$$

subject to constraint (10)

B. General case

For the general case where n fans and m positions are considered, the actual air speed, $V(P)$, generated by fans with speed setting P are given by

$$K \cdot P = V(P) \tag{12}$$

where K is an $m \times n$ gain matrix, P is an $n \times 1$ vector and V is an $m \times 1$ vector. The system represented in Eq.(12) is overdetermined if $m > n$ (more occupants than fans) and no value of P will exactly satisfy it. Therefore, it is of interest to find an approximate solution to the system, i.e., the minimax-error solution.

Substituting Eq.(12) into (1) and adding operational constraints, the minimax-error problem can be written as

$$\text{Minimize } ||K \cdot P - V_d||_\infty$$

$$\text{subject to } P_{min} < P < P_{max} \tag{13}$$

where P_{min} and P_{max} are the minimum and maximum speed settings that can be applied to the fans. The minimax-error solution P_{opt} to the problem given in (13) can be obtained by solving an equivalent linear programming problem given as

$$\text{Minimize } [0 \quad \cdots \quad 0 \quad 1]\begin{bmatrix} P \\ \varepsilon \end{bmatrix}$$

$$\text{subject to } \begin{bmatrix} I_n & 0_n \\ -I_n & 0_n \\ K & -1_m \\ -K & -1_m \end{bmatrix}\begin{bmatrix} P \\ \varepsilon \end{bmatrix} \leq \begin{bmatrix} P_{max} \\ -P_{min} \\ V_d \\ -V_d \end{bmatrix} \tag{14}$$

where I_n is an $n \times n$ identity matrix, 0_n is an $n \times 1$ vector with all entries equal to zero, 1_m is an $m \times 1$ vector with all entries equal to one, ε is a scalar, and where for vectors a and b, $a \leq b$ indicates every entry of a is no more than the corresponding entry of b. This linear programming problem can be expressed as to find a minimum ε^* that satisfies $||K \cdot P - V_d||_\infty = \varepsilon^*$, which is equivalent to the minimax-error problem stated in (13). It should be mentioned that a linear programming problem is always feasible as long as the constraint set is not empty. Sometimes there may even be multiple optimal solutions that give the same value of ε^*. In this case, we can select the one associated with the lowest power consumption.

2.2.3 Numerical optimization

In the case that the relationship between *V(P)* and *P* is nonlinear, a numerical optimization scheme can be used. Let $\hat{P}$ be the initial fan speed setting, the first-order approximation for *V(P)* around $\hat{P}$ is given by

$$V(P) \approx V(\hat{P}) + K \cdot \Delta P \tag{15}$$

where $\Delta P = P - \hat{P}$.

The gain matrix *K* can be determined by measuring $V(\hat{P}^{(1)})$ through $V(\hat{P}^{(j)})$, where each $\hat{P}^{(j)}$ is $\hat{P}$ slightly perturbed by Δp_j as follows

$$\hat{P}^{(1)} = \hat{P} + \begin{bmatrix} \Delta p_1 \\ 0 \\ 0 \\ \vdots \\ 0 \end{bmatrix}, \hat{P}^{(2)} = \hat{P} + \begin{bmatrix} 0 \\ \Delta p_2 \\ 0 \\ \vdots \\ 0 \end{bmatrix}, \cdots, \hat{P}^{(n)} = \hat{P} + \begin{bmatrix} 0 \\ 0 \\ 0 \\ \vdots \\ \Delta p_n \end{bmatrix} \tag{16}$$

and *K* can be obtained by

$$K = [k_1 \quad k_2 \quad \cdots \quad k_n] \tag{17}$$

where $k_j = \frac{V(\hat{P}^{(j)}) - V(\hat{P})}{\Delta p_j}$ is the j^{th} column of *K* and *j = 1, 2, …, n*.

Substituting Eq.(15) into (1), the optimization problem can then be formulated as

$$\text{Minimize } ||K \cdot \Delta P - \Delta V_d||_\infty$$

$$\text{subject to } -\hat{P} < \Delta P < P_{max} - \hat{P} \tag{18}$$

where $\Delta V_d = V_d - V(\hat{P})$ is the desired air speed change. The optimal fan speed setting adjustment ΔP_{opt} can be obtained by solving the following equivalent linear programming problem:

$$\text{Minimize } [0 \quad \cdots \quad 0 \quad 1] \begin{bmatrix} \Delta P \\ \varepsilon \end{bmatrix}$$

$$\text{subject to } \begin{bmatrix} I_n & 0_n \\ -I_n & 0_n \\ K & -1_m \\ -K & -1_m \end{bmatrix} \begin{bmatrix} \Delta P \\ \varepsilon \end{bmatrix} \leq \begin{bmatrix} P_{max} - \hat{P} \\ \hat{P} \\ \Delta V_d \\ -\Delta V_d \end{bmatrix} \tag{19}$$

and the optimal fan speed setting can be obtained as $P_{opt} = \hat{P} + \Delta P_{opt}$. It should be mentioned that if the relationship between *V(P)* and *P* is linear, then the optimal fan speed setting obtained from the problem in the incremental form of (19) is equivalent to the solution of the problem in the standard form of (14). The most important notations used for problem formulation are summarized in Table 1.

Table 1: Important notations used for problem formulation.

K	Pre-calibrated gain matrix, calculated by using Eq.(17) during the calibration process
ΔV_d	Desired air speed change, determined based on either the PMV – SET model or occupants' feedback
ΔP_{opt}	Optimal fan speed setting adjustment, obtained by solving problem (19)

2.3 Test scenarios

The feasibility of the proposed approach was tested in two indoor-environment scenarios in a tropical climate respectively by 1) measuring air speed directly in a business conference room and 2) involving human subject surveys in a university classroom. In these two experiments, the desired air speed was determined based on the PMV – SET model and the feedback from the occupants, respectively.

2.3.1 Experiment 1: conference room without human subjects

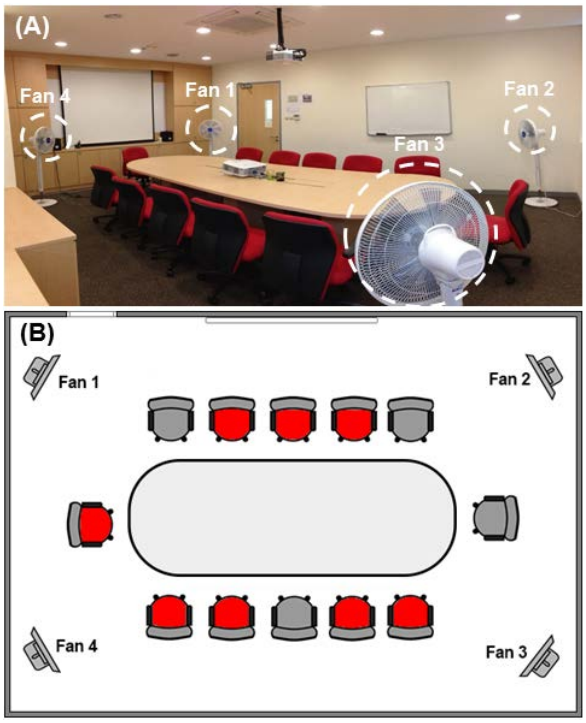

Figure 2: Experiment 1 – conference room: (A) photograph and (B) layout (red seats: occupied; grey seats: unoccupied).

In Experiment 1, the proposed approach was tested to improve the sensation of thermal comfort at target positions by providing the desired air speed determined through the PMV – SET model. The experiment was conducted in a typical conference room equipped with four DC fans. The conference room has a volume of 6.4 m × 5.0 m × 2.7 m ≈ 86.4 m^3 and is designed for reception of at most 12 occupants as shown in Figure 2. The calibration process was conducted at all 12 positions by using Eq.(17). The air speed is measured at the height of 1.1 m, which is equal to the head region of a seated person. The head region is one of the dominant body parts affecting overall comfort (Zhang et al. 2010a, Zhang et al. 2010b, Zhang et al. 2010c). The other body parts may be covered by typical office attire in the tropics (e.g., in Singapore, typical office attire includes short sleeve button or polo shirt, long trousers, socks, business shoes) and may not experience the airflow, thus being less sensitive to thermal variation. The gain matrix, K, in the test environment, was then obtained as:

$$K = [k_1 \quad k_2 \quad k_3 \quad k_4] = \begin{bmatrix} 0.0151 & 0.0035 & 0.0053 & 0.0150 \\ 0.0132 & 0.0003 & 0.0034 & 0.0082 \\ 0.0110 & 0.0062 & 0.0080 & 0.0066 \\ 0.0053 & 0.0055 & 0.0032 & 0.0028 \\ 0.0046 & 0.0072 & 0.0042 & 0.0006 \\ 0.0029 & 0.0101 & 0.0066 & 0.0005 \\ 0.0022 & 0.0138 & 0.0100 & 0.0005 \\ 0.0001 & 0.0114 & 0.0154 & 0.008 \\ 0.0017 & 0.0105 & 0.0107 & 0.0028 \\ 0.0053 & 0.0108 & 0.0096 & 0.0066 \\ 0.0098 & 0.0075 & 0.0061 & 0.0132 \\ 0.0070 & 0.0020 & 0.0002 & 0.0141 \end{bmatrix}$$

where *K* is a 12 × 4 matrix referring to 4 fans for 12 occupants. If the occupancy information is available to the system, the gain for each position will only be used when the position is occupied. To show the feasibility of the proposed approach, the 8 out of the 12 positions (red seats in Figure 2B) are assumed to be occupied in the experiment.

Three temperature levels, 26 °C, 27.5 °C and 29 °C (79 °F, 82 °F and 84 °F), were considered and the corresponding desired air speeds determined based on the PMV – SET model are given in Table 2, where relative humidity, *RH*, was assumed to be 50% and metabolic rate, *M*, was set to be 1.2 met. The details on the selection of these parameters can be found in (Liu et al. 2017).

Table 2: PMV - SET model parameters (*RH* = 50%, *M* = 1.2 met).

Temperature (°C)	Clothing	Target PMV	Desired air speed V_d (m/s)
26	0.7	0.00	0.55
27.5	0.6	0.15	0.64
29	0.5	0.30	0.78

Due to the limited coverage area by a single fan if it is set to provide unidirectional airflow and also to test our model in a more challenging condition, the fans were therefore set to be in oscillation mode during the experiment. The speed setting of each fan was initially set to 2. The optimal fan speed setting for the three temperature levels is calculated by solving the linear programming problem in (19) and the obtained results are given in Table 3. After applying the optimal results to the fans, we measured the air speed at each target position and calculated the corresponding PMV value to evaluate the thermal comfort improvement compared to the initial cases without optimization. At a sampling interval of 2 seconds, each group of measurements took 90 samples at height of 1.1 m.

Table 3: Optimized fan speed setting in Experiment 1.

Fan #	1	2	3	4
Initial case	2	2	2	2
26°C	25	18	12	11
27.5°C	32	26	16	9
29°C	32	31	22	14

2.3.2 Experiment 2: classroom with human subjects

In Experiment 2, the proposed approach was tested using human subjects. We used occupants' feedback (increasing/decreasing air speed) to determine the desired air speed. The experiment was conducted in April (the typical hot season in Singapore) in an 80-seat classroom (10.5 m × 9.5 m × 2.5 m) as shown in Figure 3A and 3B. Four HOBO data loggers for measuring air temperature and relative humidity were attached to the back of the chairs with a styofoam cushion placed in the middle. The locations of the loggers are shown as blue circles in Figure 3A.

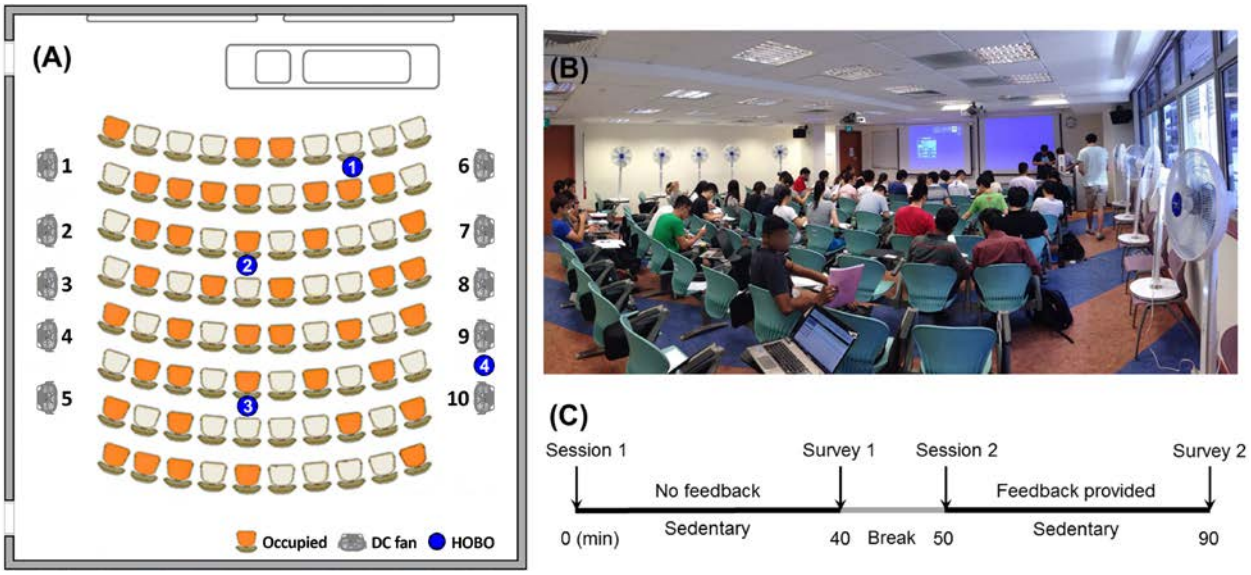

Figure 3: Experiment 2 - classroom: (A) Layout; (B) photograph of the experiment and (C) experiment procedure.

Ten DC fans were placed on both sides of the room at the height of 2 m and their speed settings can be wirelessly adjusted. A control system that can collect users' feedback through short message service was implemented. It should be mentioned that the feedback collection can also be implemented in other ways such as a smartphone app or a website.

A valid feedback message should contain the seat number and a '+'/'-' symbol to indicate the occupant's preference of increasing/decreasing air speed. The optimization algorithm running in the system then quantifies the occupants' desire to have more or less air movement by counting how many '+'/'-' symbols that each individual sends in one optimization cycle (2 min). The numbers from the count are then multiplied by a coefficient, α, to determine the desired air speed change ΔV_d in Table 1. To prevent sudden changes, α is set to 0.05 and a limit of three is imposed on each of these numbers so that the change of at most 0.05 × 3 = 0.15 m/s in air speed can be experienced by an occupant within one optimization cycle. This optimization process is repeated every 2 min and the fan speed setting is adjusted accordingly. The pseudocode of the optimization algorithm is given in Table 4.

Table 4: Pseudocode of optimization algorithm based on occupant feedback.

Parameters: $\boldsymbol{K}$ in Eq. (17), $\alpha = 0.05$
Input: Feedback.symbol, Feedback.position
Output: $\Delta \boldsymbol{P_{opt}}$
Function Optimization(Run every 2 minutes)
    n = Number of occupants
    for $i = 1 : n$
        $\Delta v_i = 0$
    end
    m = Number of received feedback in one optimization cycle
    for $j = 1 : m$
        k = Feedback(j).position
        if Feedback(j).symbol = '+'
            $\Delta v_k = \Delta v_k + 1$
        elseif Feedback(j).symbol = '-'
            $\Delta v_k = \Delta v_k - 1$
        end
        if $\Delta v_k > 3$ or $\Delta v_k < -3$
            $\Delta v_k = 3*\text{sign}(\Delta v_k)$
        end
    end
    $\Delta \boldsymbol{V_d} = \alpha*[\Delta v_{\boldsymbol{1}}, \Delta v_{\boldsymbol{2}}, \cdots, \Delta v_{\boldsymbol{n}}]^T$
    $\Delta \boldsymbol{P_{opt}} = \textit{LinearProgramming}(\boldsymbol{K}, \Delta \boldsymbol{V_d})$ in (19)
    return $\Delta \boldsymbol{P_{opt}}$
end

Forty undergraduate students (27 males, 13 females) participated in the experiment and randomly seated in the room (Figure 3B). The occupancy distribution is shown in Figure 3A. No restrictions were imposed on their clothing but most of them came with typical summer dresses (about 0.5 clo). Before the formal experiment, all the students have already attended a training session to become familiar with the experimental room, the experimental procedure, short message service-based fan control and survey questionnaires. To avoid bias in the results, all the measurements of environmental variables were not made known to the students.

The experimental procedure is shown in Figure 3C. The lecture started at 14:00 in the afternoon and for the first 40-minute session, no optimization was performed and the speed setting of each fan was initially set as 2 to avoid any discomfort. From 14:40 to 14:50, there was a break. During the second 40-minute session from 14:50 to 15:30, the students could send their feedback towards preferred air movement whenever they wanted to. The operation of the fan system was then optimized based on the feedback using the algorithm in Table 4 and the obtained optimal fan speed setting is recorded in Supplementary Information (Figure A.2). The gain matrix K used in Table 4 was obtained by pre-calibration and given in Supplementary Information (Table A.5). One limitation of this experimental design is that the magnitude of the benefits of the novel

control strategy depends on the arbitrarily selected initial speed settings. Nevertheless, thermal comfort can only be improved because the control strategy is based on occupant feedback.

The students were required to complete a survey questionnaire (Figure A.3 in Supplementary Information) at the end of each session, i.e., at 14:40 and 15:30 respectively. In the questionnaire, they recorded their conditions in a continuous scale (from -3 to 3) regarding 1) thermal acceptability, 2) thermal sensation, and 3) acceptance of air movement; and the results are given in Section 3.2. The air temperature and relative humidity were continuously measured at one-minute sampling interval during the experiment as shown in Figure 4. The details of the measurements are summarized in Supplementary Information (Table A.3).

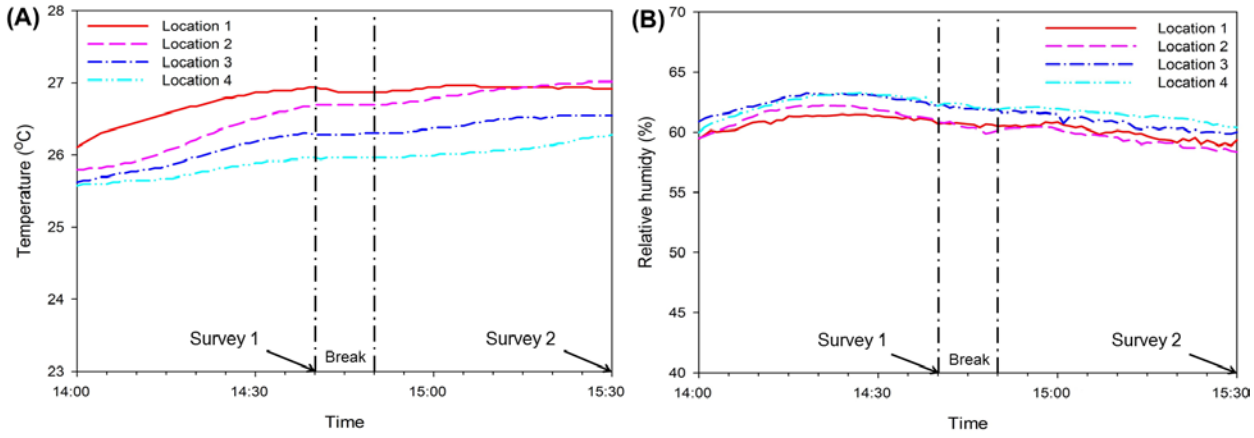

Figure 4: Measurement of environmental variables in Experiment 2: (A) air temperature and (B) relative humidity.

2.4 Statistical methods

For statistical analysis of the air speed measurements in Experiment 1 and the survey results in Experiment 2, Shapiro-Wilk test was used to test the normality of the data distribution. Paired-sample *t*-test was used for normally distributed data. Wilcoxon signed rank test was used for non-normally distributed data. Statistical significance was obtained when $p < 0.05$. Cohen's *d* (Ferguson 2009) was also employed as effect size index.

The data distributions are reported using box-and-whisker plots. The band inside the box, the bottom and top of the box are the median, 25th and 75th percentiles, respectively. The end of the whisker is the lowest/highest datum within 1.5 times the interquartile range (IQR) from the lower/upper quartile. Measurements beyond the end of a whisker are plotted as dots.

3. Results and analysis

3.1 Experiment 1: air speed measurement

The air speed measurements before and after optimization for the three temperature levels (operative temperature t_o = 26 °C, 27.5 °C and 29 °C) are shown in Figure 5. The air speed measurements do not exhibit a normal distribution ($W = 0.92$, $p < 0.001$). The medians (1st quartiles, 3rd quartiles) of all the measured data are summarized in Supplementary Information (Table A.4). Compared to the initial cases without optimization of fans operation, the proposed

approach is capable of increasing air movement towards target values thereby improving thermal comfort at higher temperatures. The improvement in air speed is statistically significant ($p < 0.001$).

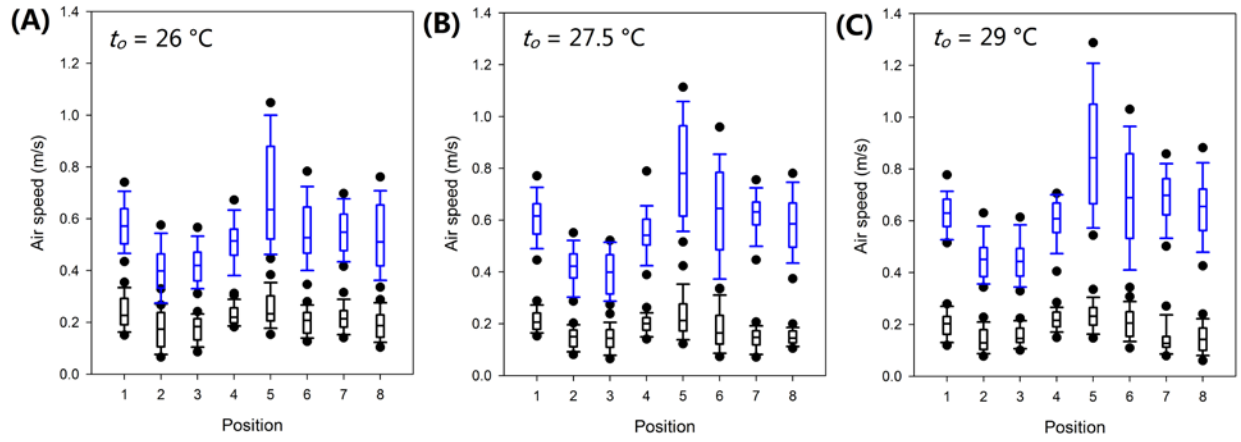

Figure 5: Air speed measurements before (black boxplots at lower row,) and after (blue boxplots at upper row) optimization: (A) t_o = 26 °C; (B) t_o = 27.5 °C and (C) t_o = 29 °C.

Since the air speed measurements do not exhibit a normal distribution, the data information in Figure 5 can be further interpreted to the plots of air speed medians in Figure 6A for easy observation. Each plot contains the medians of air speed measured at all the 8 test positions, corresponding to a column of Table A.4 in Supplementary Information. It can be seen in Figure 6A that the variance of optimized air-speed medians (right graph in blue color) becomes bigger due to the oscillated operation of fans. Nevertheless, the air speeds at test positions are closer to the desired values after being optimized.

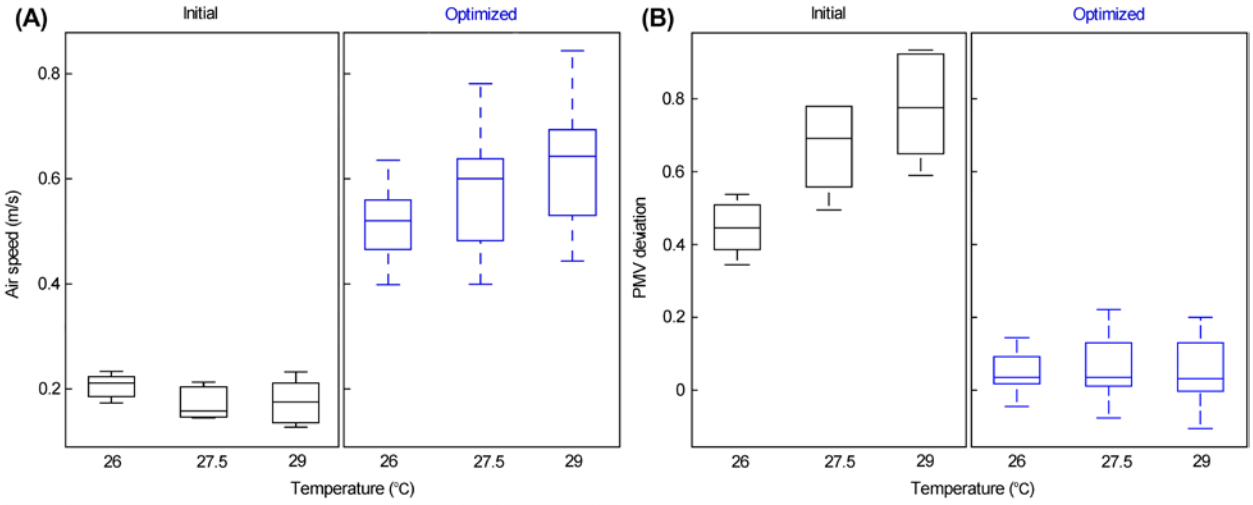

Figure 6: Comparison between initial and optimized cases: (A) medians of air speed measurements and (B) PMV deviations (actual PMV values minus target PMV values).

The actual PMV values corresponding to the air speed medians for the initial and optimized cases in Figure 6A can be calculated for thermal comfort assessment based on the PMV – SET model with the parameters in Table 2. Then it is of interest to see how far these actual PMV values are from the target ones, i.e. 0.00, 0.15 and 0.30 for 26 °C, 27.5 °C and 29 °C respectively.

To achieve this, the PMV deviations are then obtained by subtracting the target PMV values from the actual PMV values and shown in Figure 6B. For the initial cases (left graph in black color in Figure 6B), the deviations are far from zero which means the sensation of thermal comfort is quite away from our objective. On the contrary, the proposed approach is able to improve the thermal environment by keeping PMV deviations around zero for all the temperature levels considered (right graph in blue color in Figure 6B).

3.2 Experiment 2: human subject surveys

During the experiment, we received 34 valid responses from all the 40 subjects regarding thermal sensation, thermal acceptability and acceptance of air movement. Notice that Survey 1 refers to the case without the optimization of fans operation while Survey 2 refers to the case with the optimization as illustrated in Figure 3C.

Thermal sensation using the ASHRAE 7-point scale votes (from -3 = cold to +3 = hot) for the two tested conditions are shown in Figure 7A. Thermal sensation is barely normally distributed (W = 0.96, p = 0.05). In Survey 1, the median value without optimization of fans operation is 0.73 (1st quartile = 0, 3rd quartile = 1.63) and most occupants recorded their thermal sensation in the range from neutral to warm. After fans operation was kept being optimized for 40 minutes, the median value in Survey 2 decreased to -0.04 (1st quartile = -0.62, 3rd quartile = 0.13) and most occupants reported that their thermal sensation was in the range from neutral to slightly cool, which is the preferred sensation in hot and humid climates like Singapore (Gong et al. 2006). The difference is significant ($p < 0.001$) since the operation of the fans was optimized and the occupants could request higher air speed in Session 2. Compared to the descriptors for values of Cohen's d, recommended by Ferguson (2009) (where d = 0.41 refers to minimum effect size representing a practically significant effect, d = 1.15 refers to moderate effect and d = 2.70 refers to strong effect), the two groups for thermal sensation (Survey 1 and Survey 2) have a small and statistically significant difference (d = 0.96).

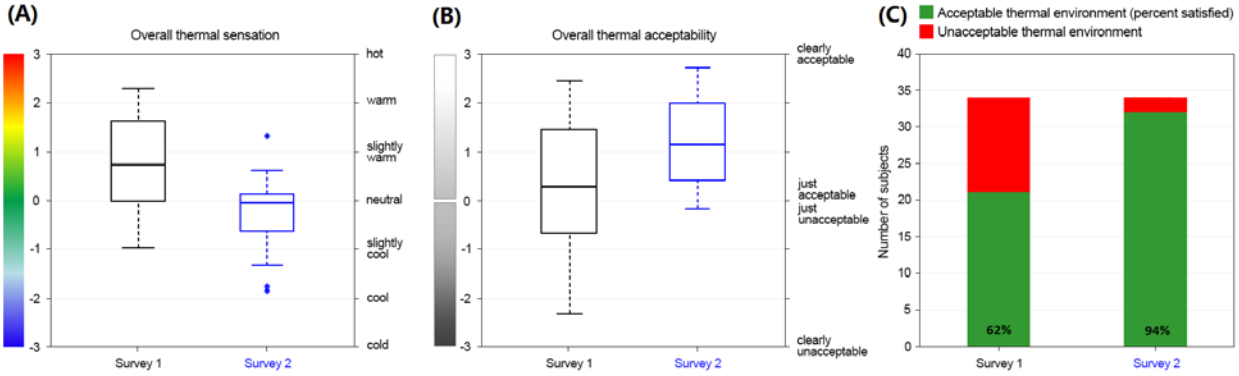

Figure 7: Thermal comfort responses for the two tested conditions: (A) overall thermal sensation; (B) overall thermal acceptability in boxplots and (C) overall thermal acceptability in bar charts (dichotomous).

Thermal acceptability votes (from -3 = clearly unacceptable to +3 = clearly acceptable) for the two tested conditions are shown in Figure 7B. Thermal acceptability is non-normally distributed (W = 0.95, p = 0.01). The median value before optimization is 0.3 (1st quartile = -0.68, 3rd quartile = 1.45) while the median value after optimization increases to 1.14 (1st quartile = 0.41,

3rd quartile = 2.00). The improvement in thermal acceptability is statistically significant (p < 0.001), and the effect size shows a moderate difference between the two groups (d = 1.24). If we look at the data in a dichotomous way (acceptable and unacceptable) as shown in Figure 7C, the percentage of students who express satisfaction with the thermal environment are 62% and 94% in Survey 1 and 2, respectively. In accordance with standards ASHRAE 55 (ANSI/ASHRAE 2013) and ISO 7730 (ISO 2005), 80% or more of the occupants should express satisfaction with the environment. It is obvious that the thermal environment does not meet the requirements when fans operation is not optimized according to occupants' feedback (Survey 1).

Acceptance of air movement votes (from -3 = clearly unacceptable to +3 = clearly acceptable) for the two tested conditions are shown in Figure 8A. Acceptance of air movement is normally distributed (W = 0.97, p = 0.18). The median acceptance of air movement is 0.27 (1st quartile = -0.55, 3rd quartile = 0.64) before optimization and 1.09 (1st quartile = 0.45, 3rd quartile = 2.00) after optimization (p < 0.001, d = 1.15). The percentages of students who express satisfaction with the air movement are 68% and 94% in Survey 1 and 2, respectively, as shown in Figure 8B. For each occupant, the score of Survey 1 is subtracted from Survey 2 and 80% of the occupants increased their vote regarding acceptance of air movement as well as thermal acceptability.

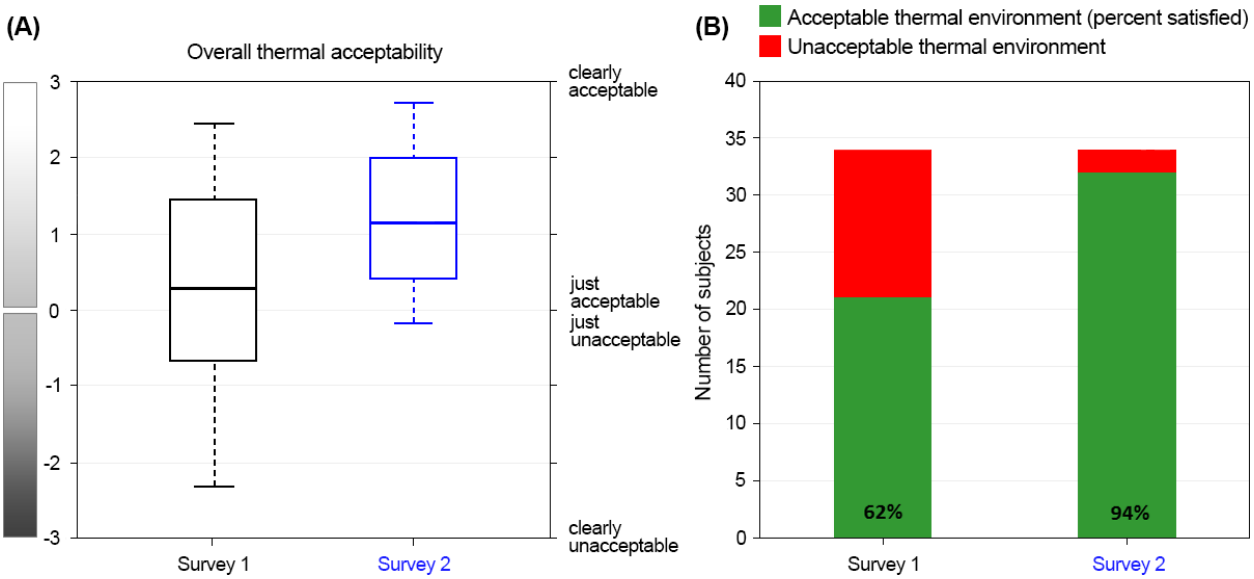

Figure 8: Overall acceptance of air movement for the two tested conditions: (A) boxplots and (B) bar charts (dichotomous).

4. Discussion

4.1 Pre-Calibration process

The proposed approach predicts airflow through a pre-calibration process by establishing a linear (or approximately linear) relationship between air speed and fan speed setting in real environments. This is a significant advantage since the airflow field generated by fans depends on many parameters (e.g., furniture layout) and now can be predicted in a cost-effective manner by using the proposed method. The pre-calibration process is also useful for determining the number of fans and their placements in the design phase. During the calibration process, the air speeds at a plurality of target positions are measured. If the measured air speeds at certain

positions are too small or too large and violate the requirement of thermal comfort, the number of fans and their relative positions will be adjusted accordingly to eliminate unsatisfactory results.

4.2 Benefits of utilizing occupancy information

The operation of a system of fans is optimized to generate the most desirable airflow for the thermal comfort of multiple occupants. This is achieved by minimizing the worst-case deviation between the actual air speed and the desired air speed. The optimization can be conducted with or without knowing the occupancy information. If occupancy information is available, only the occupied positions will be considered and the proposed method will adapt to occupancy variation by re-optimizing the fans operation. Otherwise, all the calibrated target positions will be considered. A detailed discussion of indoor positioning systems goes beyond the scope of this paper and interested readers are referred to (Liu et al. 2014, Yin et al. 2017).

4.3 Limitations and future works

The fans used in the experiments are standing DC fans, other types of fans such as ceiling fans were not tested. The experiment involving human subjects is limited by the sample size and the specific test scenario. In the future, the proposed approach can be applied to a system of ceiling fans which are more common in practice. The challenge of using ceiling fans is the interaction between airflow generated by different fans. Unlike pedestal fans, ceiling fans cannot turn and change the direction of airflow. Therefore, the placement of ceiling fans (e.g., fan-to-fan distance) is a critical factor that affects the performance of the proposed approach. Investigation of this issue is ongoing.

In the experiment, a centralized control strategy is employed for the fan system and the failure of the central controller may cause a crash of the whole system. In practice, distributed optimization techniques (Ye & Hu 2016) can be applied to address this issue. Apart from occupants' feedback and PMV–SET model, the desired air speed can also be controlled by novel personal comfort models (Kim et al. 2018), including the one based on physiological signals like skin temperature (Choi et al. 2012, Ghahramani et al. 2017, Cheng et al. 2017). In addition, it would be interesting to coordinate the system of fans with the air conditioning and mechanical ventilation (ACMV) system for energy conservation and thermal comfort.

5. Conclusion

In this paper, a novel cooperative control approach for a system of fans is proposed to improve thermal comfort and save energy. The airflow is predicted in a cost-effective manner by using a linear relationship between air speed and fan speed setting obtained from a pre-calibration process. The fans operation is then optimized to minimize the worst-case deviation from the desired air speed, which can be determined based on either the PMV – SET model or the occupants' feedback regarding their preferences of air movement.

The proposed method was tested in two indoor environment experiments. In Experiment 1, the measured air speeds after optimization are closer to the target values indicating improved thermal comfort. In Experiment 2, occupant thermal satisfaction and air movement acceptability

increased from 62% to 94% and from 68% to 92%, respectively, after optimization was performed.

These results show that the proposed method is able to control a system of electric fans effectively to improve thermal comfort with higher cooling setpoints for energy savings. It can be applied in air-conditioned spaces such as offices, theaters or classrooms to assist air conditioning system with a higher cooling setpoint or non-air-conditioned spaces such as hawker centers (open-air food centers) where the fans conventionally operate at a predetermined speed setting.

Acknowledgment

This research is funded by the Republic of Singapore's National Research Foundation through a grant to the Berkeley Education Alliance for Research in Singapore (BEARS) for the Singapore-Berkeley Building Efficiency and Sustainability in the Tropics (SinBerBEST) Program. BEARS has been established by the University of California, Berkeley as a center for intellectual excellence in research and education in Singapore.

Reference

[1] ANSI/ASHRAE (2013). ANSI/ASHRAE Standard 55-2013, Thermal environmental conditions for human occupancy. *Atlanta, USA: American Society of Heating, Refrigerating and Air-Conditioning Engineers*.

[2] Arens, E., Stephen Turner, P. E., & Zhang, H. (2009). Moving air for comfort. *ASHRAE Journal*, *51*(5), 18–29.

[3] Babich, F., Cook, M., Loveday, D., Rawal, R., Shukla, Y., (2017). Transient three-dimensional CFD modelling of ceiling fans. *Building and Environment*. 123, 37–49.

[4] Cândido, C., de Dear, R., & Lamberts, R. (2011). Combined thermal acceptability and air movement assessments in a hot humid climate. *Building and Environment*, *46*(2), 379–385.

[5] Cheng, R. (1993). *U.S. Patent No. 5,197,858. Washington, DC: U.S. Patent and Trademark Office*.

[6] Cheng, X., Yang, B., Olofsson, T., Liu, G., & Li, H. (2017). A pilot study of online non-invasive measuring technology based on video magnification to determine skin temperature. *Building and Environment*, 121, 1–10.

[7] Choi, J. H., & Loftness, V. (2012). Investigation of human body skin temperatures as a bio-signal to indicate overall thermal sensations. *Building and Environment*, *58*, 258-269

[8] DOE (2011). 2011 Building energy data book. *United States Department of Energy, Washington, DC*.

[9] Duarte, C., Raftery, P., & Schiavon, S. (2017). Development of whole building energy models for detailed energy insights of a large office building with green certification rating in Singapore. *Energy Technology*. https://doi.org/10.1002/ente.201700564.

[10] EMA (2015). Singapore energy statistics 2015. *Energy Market Authority Singapore*.

[11] Fanger, P. O. (1970). Thermal comfort. Analysis and applications in environmental engineering. *Copenhagen: Danish Technical Press.*

[12] Ferguson, C. J. (2009). An effect size primer: A guide for clinicians and researchers. *Professional Psychology: Research and Practice*, *40*(5), 532.

[13] Gagge, A. P. (1971). An effective temperature scale based on a simple model of human physiological regulatory response. *ASHRAE Trans., 77*, 247-262.
[14] Ghahramani, A., Castro, G., Becerik-Gerber, B., & Yu, X. (2016). Infrared thermography of human face for monitoring thermoregulation performance and estimating personal thermal comfort. *Building and Environment*, *109*, 1-11.
[15] Gluszek, A., & Gluszek, J. M. (1995). *U.S. Patent No. 5,449,275*. *Washington, DC: U.S. Patent and Trademark Office*.
[16] Gong, N., Tham, K. W., Melikov, A. K., Wyon, D. P., Sekhar, S. C., & Cheong, K. W. (2006). The acceptable air velocity range for local air movement in the tropics. *HVAC&R Research*, *12*(4), 1065-1076.
[17] Hoyt, T., Arens, E., & Zhang, H. (2015). Extending air temperature setpoints: Simulated energy savings and design considerations for new and retrofit buildings. *Building and Environment*, *88*, 89-96.
[18] Huang, L., Ouyang, Q., Zhu, Y., & Jiang, L. (2013). A study about the demand for air movement in warm environment. *Building and Environment*, *61*, 27–33.
[19] ISO (2005). ISO 7730:2005, Ergonomics of the thermal environment, Analytical determination and interpretation of thermal comfort using calculation of the PMV and PPD indices and local thermal comfort criteria. *Geneva: International Organization for Standardization*.
[20] Khalil, E. E., & Abou Zeid, A. (2016). Comparative Assessment of Air Distribution Systems: Improving Indoor Thermal Comfort in Office Spaces. In *54th AIAA Aerospace Sciences Meeting* (p. 1364).
[21] Kim, J., Schiavon, S., & Brager, G. (2018). Personal comfort models–A new paradigm in thermal comfort for occupant-centric environmental control. *Building and Environment*, January 2018. https://doi.org/10.1016/j.buildenv.2018.01.023.
[22] Kolarik, J., Toftum, J., Olesen, B. W., & Jensen, K. L. (2011). Simulation of energy use, human thermal comfort and office work performance in buildings with moderately drifting operative temperatures. *Energy and Buildings*, *43*(11), 2988–2997.
[23] Liu, S., Yin, L., Ho, W. K., & Ling, K. V. (2014). Improved indoor tracking based on generalized t-distribution noise model. In *Control Automation Robotics & Vision (ICARCV), 2014 13th International Conference on* (pp. 687-692). IEEE.
[24] Liu, S., Yin, L., Ho, W. K., Ling, K. V., & Schiavon, S. (2017). A tracking cooling fan using geofence and camera-based indoor localization. *Building and Environment*, *114*, 36-44.
[25] Momoi, Y., Sagara, K., Yamanaka, T., Kotani, H., 2004. Modeling of ceiling fan based on velocity measurement for CFD simulation of airflow in large room. The 9th International Conference on Air Distribution in Rooms, Coimbra, Portugal, pp. 145–150.
[26] NEA (2010). Singapore's second national communication: under the United Nations framework convention on climate change. *National Environment Agency, Republic of Singapore*.
[27] Norman, S. A. (1991). Optimization of wafer temperature uniformity in rapid thermal processing systems. *IEEE Transactions on Electron Devices*, 1-46.
[28] Pérez-Lombard, L., Ortiz, J., & Pout, C. (2008). A review on buildings energy consumption information. *Energy and Buildings*, *40*(3), 394-398.
[29] Posner, J. D., Buchanan, C. R., & Dunn-Rankin, D. (2003). Measurement and prediction of indoor air flow in a model room. *Energy and Buildings*, *35*(5), 515-526.
[30] Rim, D., Schiavon, S., & Nazaroff, W. W. (2015). Energy and cost associated with ventilating office buildings in a tropical climate. *PloS One*, *10*(3), e0122310.

[31] Schiavon, S., & Melikov, A. K. (2008). Energy saving and improved comfort by increased air movement. *Energy and Buildings*, *40*(10), 1954-1960.
[32] Schiavon, S., Hoyt, T., & Piccioli, A. (2014). Web application for thermal comfort visualization and calculation according to ASHRAE Standard 55. *Building Simulation*, *7*(4), 321–334.
[33] Schiavon, S., Yang, B., Donner, Y., Chang, V. C., & Nazaroff, W. W. (2017). Thermal comfort, perceived air quality, and cognitive performance when personally controlled air movement is used by tropically acclimatized persons. Indoor air, 27(3), 690-702.
[34] Sekhar, S. C. (1995). Higher space temperatures and better thermal comfort—a tropical analysis. *Energy and Buildings*, 23(1), 63-70.
[35] Shahzad, S., Brennan, J., Theodossopoulos, D., Hughes, B., & Calautit, J. K. (2017). Energy and comfort in contemporary open plan and traditional personal offices. *Applied Energy*, *185*, *Part 2*, 1542–1555.
[36] Xu, Z., Liu, S., Hu, G., & Spanos, C. J. (2017). Optimal coordination of air conditioning system and personal fans for building energy efficiency improvement. *Energy and Buildings*, *141*, 308-320.
[37] Yang, B., Schiavon, S., Sekhar, C., Cheong, D., Tham, K. W., & Nazaroff, W. W. (2015). Cooling efficiency of a brushless direct current stand fan. *Building and Environment*, *85*, 196-204.
[38] Yang, B., & Olofsson, T. (2017). A questionnaire survey on sleeping environment conditioned by different cooling modes in multistory residential buildings of Singapore. *Indoor and Built Environment*, 26(1), 21─31.
[39] Ye, M., & Hu, G. (2016). Distributed extremum seeking for constrained networked optimization and its application to energy consumption control in smart grid. *IEEE Transactions on Control Systems Technology*, 24(6), 2048-2058.
[40] Yin, L., Liu, S., Ho, W. K., & Ling, K. V. (2017). Indoor tracking with the generalized t-distribution noise model. *IEEE Transactions on Control Systems Technology*. DOI: 10.1109/TCST.2017.2692737.
[41] Zhai, Z. J., Zhang, Z., Zhang, W., & Chen, Q. Y. (2007). Evaluation of various turbulence models in predicting airflow and turbulence in enclosed environments by CFD: Part 1—Summary of prevalent turbulence models. *HVAC&R Research*, *13*(6), 853-870.
[42] Zhai, Y., Zhang, H., Zhang, Y., Pasut, W., Arens, E., & Meng, Q. (2013). Comfort under personally controlled air movement in warm and humid environments. *Building and Environment*, *65*, 109-117.
[43] Zhang, Z., Zhang, W., Zhai, Z. J., & Chen, Q. Y. (2007). Evaluation of various turbulence models in predicting airflow and turbulence in enclosed environments by CFD: Part 2—Comparison with experimental data from literature. *HVAC&R Research*, *13*(6), 871-886.
[44] Zhang, H., Arens, E., Huizenga, C., & Han T. (2010a). Thermal sensation and comfort models for non-uniform and transient environments, Part I: local sensation of individual body parts. *Building and Environment* 45, no. 2, 380–388.
[45] Zhang, H., Arens, E., Huizenga, C., & Han T. (2010b). Thermal sensation and comfort models for non-uniform and transient environments, Part II: local comfort of individual body parts. *Building and Environment* 45, no. 2, 389–398.
[46] Zhang, H., Arens, E., Huizenga, C., & Han T. (2010c). Thermal sensation and comfort models for non-uniform and transient environments, Part III: whole-body sensation and comfort. *Building and Environment* 45, no. 2, 399–410.

Supplementary Information

Table A.1: Fan speed setting, fan power and corresponding air speed at tested distance.

Speed setting	Power (W)	Average air speed (m/s)							
		0.5 m	1.0 m	1.5 m	2.0 m	2.5 m	3.0 m	3.5 m	4.0 m
1	3.8	0.96	0.77	0.67	0.58	0.46	0.39	0.32	0.31
2	4.4	1.13	0.93	0.81	0.69	0.54	0.46	0.38	0.37
3	4.7	1.30	1.07	0.94	0.79	0.65	0.57	0.46	0.44
4	5.2	1.51	1.20	1.03	0.85	0.72	0.66	0.54	0.51
5	5.7	1.67	1.29	1.12	0.92	0.79	0.72	0.57	0.55
6	6.4	1.79	1.38	1.18	0.96	0.84	0.76	0.59	0.58
7	6.8	1.87	1.44	1.24	1.01	0.85	0.76	0.60	0.59
8	7.9	2.06	1.53	1.32	1.06	0.94	0.84	0.68	0.64
9	8.6	2.21	1.64	1.42	1.17	0.98	0.90	0.73	0.69
10	9.1	2.21	1.66	1.45	1.21	1.00	0.91	0.75	0.71
11	9.6	2.33	1.73	1.50	1.24	1.02	0.92	0.75	0.69
12	10.9	2.44	1.81	1.59	1.31	1.04	0.95	0.80	0.73
13	11.8	2.56	1.87	1.63	1.35	1.13	1.03	0.84	0.78
14	13.0	2.57	1.85	1.63	1.38	1.14	1.02	0.83	0.77
15	14.2	2.82	2.00	1.76	1.45	1.16	1.04	0.89	0.80
16	15.4	2.90	2.05	1.80	1.48	1.28	1.13	0.95	0.85
17	16.4	3.02	2.11	1.88	1.59	1.33	1.19	1.02	0.92
18	17.6	2.98	2.11	1.89	1.58	1.30	1.16	1.00	0.90
19	18.4	2.98	2.05	1.85	1.58	1.32	1.17	0.99	0.85
20	19.3	3.04	2.15	1.93	1.63	1.37	1.22	1.06	0.93
21	19.9	3.30	2.28	2.05	1.69	1.22	1.09	0.93	0.81
22	20.6	3.35	2.29	2.07	1.73	1.35	1.21	1.03	0.92
23	21.2	3.22	2.14	1.96	1.68	1.35	1.22	1.01	0.87
24	22.4	3.55	2.36	2.12	1.77	1.27	1.12	0.96	0.84
25	23.2	3.40	2.30	2.05	1.74	1.34	1.19	1.01	0.88
26	24.1	3.58	2.39	2.16	1.83	1.45	1.29	1.08	0.96
27	25.2	3.69	2.49	2.24	1.86	1.38	1.25	1.08	0.95
28	26.0	3.78	2.52	2.26	1.87	1.47	1.33	1.12	0.99
29	27.3	3.82	2.58	2.29	1.90	1.45	1.30	1.11	1.00
30	29.2	3.98	2.60	2.32	1.96	1.57	1.41	1.18	1.04
31	30.9	4.10	2.69	2.39	1.96	1.54	1.39	1.21	1.03
32	32.5	4.20	2.78	2.46	2.01	1.37	1.25	1.00	0.98

We verified that air speed could be a natural logarithm function of fan power in previous research (Yang et al. 2015, Liu et al. 2017). Nevertheless, it is more convenient and easier to adjust the fan speed setting directly instead of fan power as this tuning function is available for most of the fans in the market. Therefore, we verified the relationship between air speed and fan speed setting which is assumed to be linear in Eq.(12). As a comparison, a natural logarithm relationship was also tested.

During the measurement process, the axis of the fan blades and motor, and the sensor were placed at 1.1 m above the ground, referring to the head height of a seated person. The measuring sensor was situated at one of eight positions with a certain distance away from the fan: from 0.5 m to 4.0 m in a distance grid of 0.5 m. At each position, the air speed generated by the fan was measured accordingly when the speed setting of the fan was increased from 1 to 32 with a step of 1. For each speed setting, 90 samples of air speed were taken and the average value was used to fit a curve at this distance by means of the least-squares algorithm. The fan speed setting, fan power and their corresponding air speed at each distance are given in Table A.1.

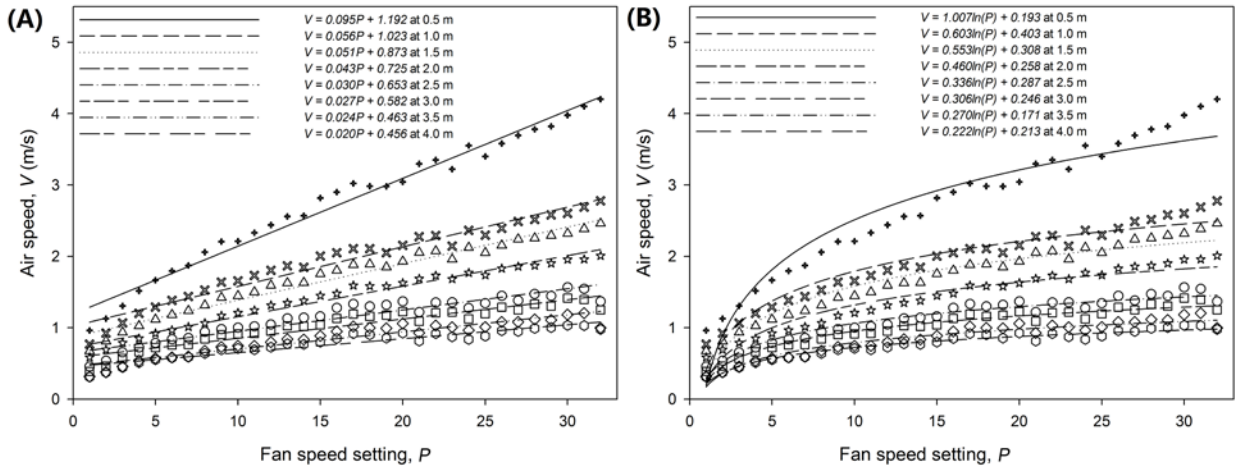

Figure A.1: Models between air speed and fan speed setting: (A) linear model; (B) natural logarithm model.

The fitted curves for both linear and natural logarithm models at selected distances are plotted in Figure A.1A and A.1B respectively, where the average values of measured air speed are shown as scatter plots. It can be seen in Figure A.1B that the logarithm model fails to represent the measured air speed well enough at nearer distances, e.g., at the distance of 0.5 m. The two models can then be compared by calculating the mean absolute error e_{ma} and the root means square error e_{rms} between the measured air speed and the fitted curve, which are summarized in Table A.2. At nearer positions up to 2 m, the straight lines fit the measured data better than the logarithmic curves. Especially, at the distance of 0.5 m, the errors e_{ma} and e_{rms} can be as high as 0.21 m/s and 0.26 m/s respectively for the natural logarithm model, which is unacceptable. Even though at farther distances beyond 2.5 m, the errors of the straight lines are slightly bigger than those of the logarithm curves, they are still limited within 0.1 m/s which is good enough for the application. In a summary, the assumed linear relationship between air speed and fan speed setting is valid.

Table A.2: Errors between measured air speed and fitted curves.

Distance (m)	Linear model	Natural logarithm model

	e_{ma} (m/s)	e_{rms} (m/s)	e_{ma} (m/s)	e_{rms} (m/s)
0.5	0.11	0.13	0.21	0.26
1.0	0.09	0.11	0.10	0.13
1.5	0.07	0.09	0.10	0.12
2.0	0.06	0.07	0.08	0.10
2.5	0.08	0.10	0.06	0.07
3.0	0.07	0.09	0.05	0.06
3.5	0.06	0.08	0.05	0.06
4.0	0.05	0.07	0.04	0.04

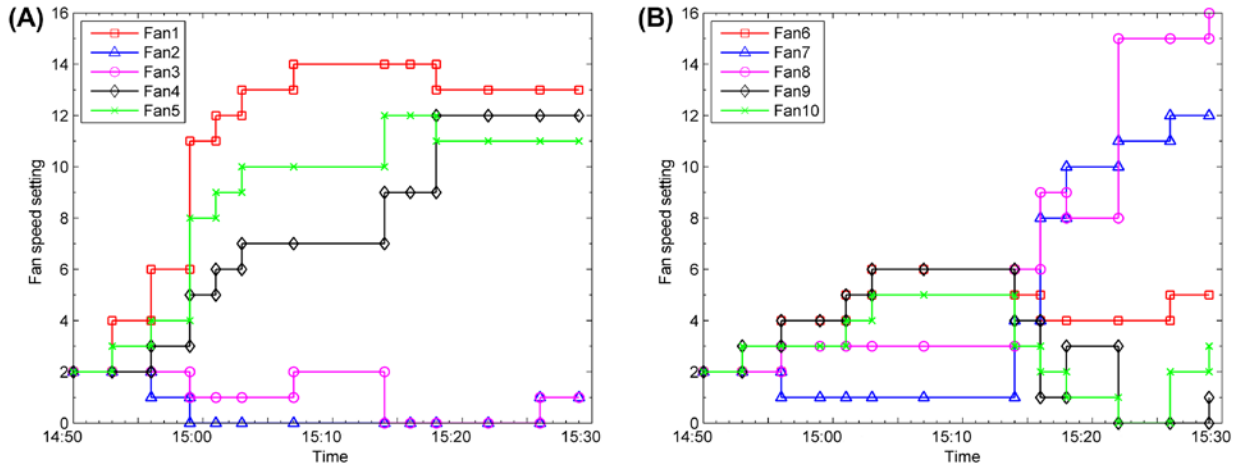

Figure A.2: Fan speed setting obtained by the algorithm in Table 4: (A) Fan 1 to 5 and (B) Fan 6 to 10.

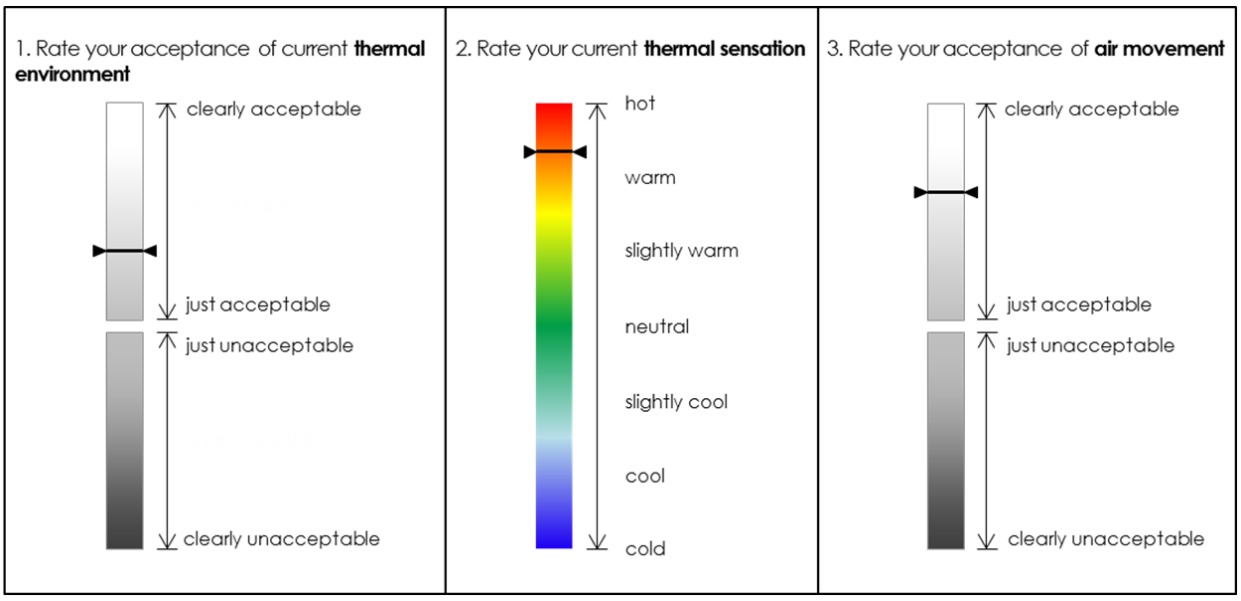

Figure A.3: Survey questionnaire in Experiment 2.

Table A.3: Measured air temperature and relative humidity in Figure 4.

Location	Air temperature (°C)			Relative humidity (%)		
	Session 1	Session 2	Overall	Session 1	Session 2	Overall
1	26.6±0.2	26.9±0.1	26.8±0.2	61.0±0.5	60.0±0.6	60.5±0.7
2	26.2±0.3	26.9±0.1	26.6±0.4	61.5±0.8	59.5±0.7	60.5±1.2
3	26.0±0.2	26.4±0.1	26.2±0.3	62.5±0.6	60.8±0.6	61.7±1.0
4	25.8±0.1	26.1±0.1	25.9±0.2	62.4±0.9	61.4±0.5	62.0±0.8
Overall	26.1±0.4	26.6±0.4	26.4±0.4	61.8±1.0	60.4±1.0	61.1±1.2

Table A.4: Medians (1st quartiles, 3rd quartiles) of air speed measurement in m/s in Figure 5.

Test positions	26 °C		27.5 °C		29 °C	
	Initial	Optimized	Initial	Optimized	Initial	Optimized
1	0.23 (0.19,0.29)	0.57 (0.50,0.64)	0.21 (0.18,0.24)	0.62 (0.55,0.66)	0.20 (0.16,0.23)	0.63 (0.58,0.68)
2	0.17 (0.11,0.24)	0.40 (0.33,0.46)	0.15 (0.11,0.18)	0.42 (0.38,0.47)	0.13 (0.10,0.18)	0.45 (0.39,0.49)
3	0.18 (0.13,0.21)	0.42 (0.36,0.47)	0.14 (0.11,0.18)	0.40 (0.32,0.47)	0.15 (0.13,0.19)	0.44 (0.39,0.49)
4	0.22 (0.20,0.26)	0.51 (0.46,0.56)	0.20 (0.18,0.22)	0.54 (0.51,0.60)	0.22 (0.19,0.25)	0.61 (0.56,0.67)
5	0.23 (0.21,0.30)	0.64 (0.52,0.88)	0.21 (0.17,0.28)	0.78 (0.62,0.96)	0.23 (0.20,0.27)	0.84 (0.67,1.05)
6	0.21 (0.16,0.24)	0.53 (0.47,0.64)	0.16 (0.12,0.23)	0.64 (0.49,0.78)	0.21 (0.15,0.25)	0.69 (0.54,0.86)
7	0.21 (0.18,0.25)	0.55 (0.48,0.62)	0.15 (0.12,0.17)	0.63 (0.58,0.67)	0.13 (0.11,0.15)	0.70 (0.62,0.76)
8	0.19 (0.14,0.23)	0.51 (0.42,0.65)	0.14 (0.13,0.17)	0.59 (0.50,0.67)	0.14 (0.10,0.19)	0.66 (0.56,0.72)

Table A.5: Gain matrix $K_{80\times10}$ in Experiment 2

0.0140	0.0010	0	0	0	0	0	0	0	0
0.0123	0.0010	0	0	0	0	0	0	0	0
0.0100	0.0020	0	0	0	0.0020	0	0	0	0
0.0090	0.0020	0	0	0	0.0030	0	0	0	0
0.0060	0.0010	0	0	0	0.0040	0	0	0	0
0.0040	0	0	0	0	0.0060	0.0010	0	0	0
0.0030	0	0	0	0	0.0090	0.0020	0	0	0
0.0020	0	0	0	0	0.0100	0.0020	0	0	0
0	0	0	0	0	0.0123	0.0010	0	0	0
0	0	0	0	0	0.0140	0.0010	0	0	0
0.0165	0.0084	0	0	0	0	0	0	0	0
0.0157	0.0064	0	0	0	0	0	0	0	0
0.0145	0.0064	0	0	0	0.0020	0	0	0	0
0.0131	0.0062	0.0013	0	0	0.0050	0	0	0	0
0.0111	0.0043	0.0013	0	0	0.0080	0.0020	0	0	0
0.0080	0.0020	0	0	0	0.0111	0.0043	0.0013	0	0
0.0050	0	0	0	0	0.0131	0.0062	0.0013	0	0
0.0020	0	0	0	0	0.0145	0.0084	0	0	0
0	0	0	0	0	0.0157	0.0084	0	0	0
0	0	0	0	0	0.0165	0.0104	0	0	0
0.0165	0.0140	0.0070	0	0	0	0	0	0	0
0.0158	0.0127	0.0080	0	0	0	0	0	0	0
0.0139	0.0105	0.0060	0	0	0	0.0020	0	0	0
0.0136	0.0090	0.0050	0.0010	0	0.0010	0.0030	0	0	0
0.0105	0.0070	0.0030	0.0010	0	0.0050	0.0050	0.0020	0	0
0.0050	0.0050	0.0010	0	0	0.0105	0.0070	0.0040	0.0010	0
0.0010	0.0030	0	0	0	0.0136	0.0090	0.0060	0.0010	0
0	0.0020	0	0	0	0.0139	0.0105	0.0060	0	0
0	0	0	0	0	0.0158	0.0107	0.0070	0	0
0	0	0	0	0	0.0165	0.0100	0.0070	0	0
0.0120	0.0160	0.0153	0.0080	0.0007	0	0	0	0	0
0.0102	0.0142	0.0138	0.0080	0.0012	0	0	0	0	0
0.0083	0.0130	0.0119	0.0069	0.0013	0	0.0010	0.0020	0	0
0.0060	0.0101	0.0100	0.0050	0.0016	0	0.0030	0.0040	0.0010	0
0.0044	0.0090	0.0080	0.0041	0.0012	0.0020	0.0050	0.0060	0.0030	0.0010
0.0020	0.0070	0.0060	0.0020	0.0010	0.0044	0.0070	0.0080	0.0041	0.0012
0	0.0050	0.0040	0.0010	0	0.0060	0.0081	0.0100	0.0050	0.0016
0	0.0020	0.0020	0	0	0.0083	0.0100	0.0119	0.0069	0.0013
0	0	0	0	0	0.0082	0.0122	0.0138	0.0070	0.0012
0	0	0	0	0	0.0100	0.0140	0.0153	0.0060	0.0007
0.0080	0.0140	0.0160	0.0140	0.0080	0	0	0	0	0
0.0067	0.0133	0.0145	0.0134	0.0080	0	0	0	0	0

0.0044	0.0111	0.0134	0.0126	0.0069	0	0	0.0020	0.0010	0
0.0030	0.0101	0.0104	0.0106	0.0050	0	0.0020	0.0040	0.0030	0.0010
0.0023	0.0080	0.0080	0.0090	0.0041	0.0013	0.0050	0.0060	0.0070	0.0030
0.0013	0.0050	0.0060	0.0070	0.0030	0.0023	0.0080	0.0080	0.0090	0.0041
0	0.0020	0.0040	0.0030	0.0010	0.0030	0.0101	0.0104	0.0106	0.0050
0	0	0.0020	0.0010	0	0.0034	0.0101	0.0134	0.0126	0.0069
0	0	0	0	0	0.0047	0.0133	0.0145	0.0134	0.0080
0	0	0	0	0	0.0030	0.0100	0.0160	0.0140	0.0080
0.0010	0.0070	0.0130	0.0160	0.0140	0	0	0	0	0
0.0010	0.0080	0.0117	0.0149	0.0134	0	0	0	0	0
0.0010	0.0080	0.0100	0.0134	0.0126	0	0	0	0.0040	0.0010
0.0010	0.0070	0.0080	0.0122	0.0106	0	0	0.0020	0.0060	0.0030
0	0.0050	0.0060	0.0100	0.0090	0	0.0030	0.0040	0.0080	0.0070
0	0.0030	0.0040	0.0080	0.0070	0	0.0080	0.0060	0.0100	0.0090
0	0	0.0020	0.0060	0.0030	0	0.0080	0.0090	0.0122	0.0106
0	0	0	0.0040	0.0010	0	0.0070	0.0110	0.0134	0.0126
0	0	0	0	0	0	0.0060	0.0127	0.0149	0.0134
0	0	0	0	0	0	0.0040	0.0110	0.0160	0.0140
0	0	0.0080	0.0140	0.0160	0	0	0	0	0
0	0	0.0070	0.0131	0.0149	0	0	0	0	0
0	0	0.0070	0.0115	0.0134	0	0	0	0	0.0040
0	0.0013	0.0064	0.0094	0.0122	0	0	0.0010	0.0020	0.0060
0	0.0017	0.0056	0.0073	0.0100	0	0	0.0030	0.0040	0.0080
0	0	0.0030	0.0040	0.0080	0	0.0017	0.0056	0.0083	0.0100
0	0	0.0010	0.0020	0.0060	0	0.0013	0.0064	0.0104	0.0122
0	0	0	0	0.0040	0	0	0.0070	0.0115	0.0134
0	0	0	0	0	0	0	0.0050	0.0131	0.0149
0	0	0	0	0	0	0	0.0030	0.0140	0.0160
0	0	0.0010	0.0040	0.0140	0	0	0	0	0
0	0	0.0012	0.0070	0.0131	0	0	0	0	0
0	0	0.0024	0.0080	0.0115	0	0	0	0	0
0	0	0.0021	0.0061	0.0104	0	0	0	0	0.0020
0	0	0.0022	0.0040	0.0083	0	0	0.0010	0.0010	0.0040
0	0	0.0010	0.0010	0.0040	0	0	0.0022	0.0020	0.0083
0	0	0	0	0.0020	0	0	0.0021	0.0041	0.0104
0	0	0	0	0	0	0	0.0014	0.0080	0.0115
0	0	0	0	0	0	0	0.0012	0.0070	0.0131
0	0	0	0	0	0	0	0.0010	0.0030	0.0140